Recombinant Human Soluble Thrombomodulin Suppresses Arteritis in a Mouse Model of Kawasaki Disease

Hironobu Nakayama (nakayamh@suzuka-u.ac.jp)
Suzuka University of Medical Science: Suzuka Iryo Kagaku Daigaku https://orcid.org/0000-0001-7444-1173

Hiroyasu Inada
Suzuka University of Medical Science: Suzuka Iryo Kagaku Daigaku

Tatsuya Inukai
Tokyo Medical University: Tokyo Ika Daigaku

Kenta Kondo
Suzuka Kaisei Hospital

Kazuyuki Hirai
Suzuka University of Medical Science: Suzuka Iryo Kagaku Daigaku

Tomonari Tsutsumi
Suzuka University of Medical Science: Suzuka Iryo Kagaku Daigaku

Yoshiyuki Adachi
Tokyo University of Pharmacy and Life Science: Tokyo Yakka Daigaku

Noriko Nagi-Miura
Tokyo University of Pharmacy and Life Science: Tokyo Yakka Daigaku

Naohito Ohno
Tokyo University of Pharmacy and Life Science: Tokyo Yakka Daigaku

Koji Suzuki
Suzuka University of Medical Science: Suzuka Iryo Kagaku Daigaku

Research Article

Keywords: Kawasaki disease, recombinant human soluble thrombomodulin (rTM), anti-inflammatory function, vasculitis, Candida albicans water-soluble fraction (CAWS)

Posted Date: March 19th, 2021

DOI: https://doi.org/10.21203/rs.3.rs-304406/v1

Version of Record: A version of this preprint was published at Journal of Vascular Research on December 20th, 2021. See the published version at https://doi.org/10.1159/000520717.

Abstract

Background: Kawasaki Disease (KD) is associated with diffuse and systemic vasculitis of unknown aetiology and mainly affects infants and children. Intravenous immunoglobulin (IVIG) treatment reduces the risk of developing coronary aneurysms, but some children have IVIG-resistant KD, and they are at an increased risk of developing coronary artery injury. Here, we investigated the effect of recombinant human soluble thrombomodulin (rTM), which has anticoagulation, anti-inflammatory and cytoprotective properties, on the development of coronary arteritis in a mouse model of vasculitis.

Methods: To prepare an animal model of KD-like vasculitis, *Candida albicans* water-soluble fraction (CAWS) was intraperitoneally injected into DBA/2 mice for 5 consecutive days, and then rTM (0, 0.2, 1, and 4 mg/kg body weight) was injected. rTM administration was performed at two intervals: one is for 10 consecutive days from the first day and the other is for 5 consecutive days from the 1st to 15th days. Histopathological analysis of the heart was performed 20, 27, 34, and 48 days after CAWS treatment, and the gene expression of anti-inflammatory cytokine interleukin-10 (IL-10), pro-inflammatory cytokine tumor necrosis factor alpha (TNF-α), and tissue factor (TF) in the heart and spleen was investigated.

Results: Five consecutive doses of rTM (4 mg/kg) from 1 to 14 days after CAWS treatment significantly suppressed cardiac hypertrophy and arteritis by 34 days after CAWS treatment. The gene expression analysis of samples prepared from the heart and spleen of mice treated with CAWS and/or rTM showed that rTM administration increased the level of IL-10 in the heart. This increase was observed until day 27 and was not observed thereafter. The expression of TNF-α was observed in the heart of mice treated with CAWS and was not altered by rTM treatment. However, in the spleen, CAWS treatment reduced the IL-10 level and increased the TF level, whereas rTM treatment restored normal levels of both factors.

Conclusions: These findings suggest that rTM specifically increases IL-10, decreases TF, and suppresses CAWS-induced vasculitis without affecting TNF-α production. Therefore, rTM can be used as a treatment for KD.

Background

Kawasaki disease (KD), an acute febrile multisystem vasculitis, is the most common cause of acquired cardiac disease in children [1]. The incidence of KD continues to increase despite the decline in child population. In addition, the number of KD types that do not completely adapt to the diagnostic criteria is also increasing. When untreated, coronary aneurysms occur in approximately 25% of the patients, and they have been reported to contribute to the development of cardiovascular disease in adults [2–4]. The aetiology of KD remains unknown, but high-dose intravenous immunoglobulin therapy (IVIG therapy) is the first-line treatment strategy against KD, reducing the incidence of coronary aneurysm from 25–1%–5% [2–4]. However, KD refractory to IVIG therapy is recognised in approximately 10–20% of patients and cardiovascular sequelae in 2–3% of patients. Most paediatricians prescribe additional courses of IVIG,

steroids, or infliximab, and anti-tumour necrosis factor alpha (TNF-α) drugs [2–4]. However, the effectiveness of these agents in controlling coronary arteritis has not yet been established [5].

Although no aetiological factors related to KD have been identified, epidemiological evidence suggests that environmental factors may contribute to KD susceptibility and severity, taking into consideration the seasonal variations in KD development [6]. Recently, Rodó et al. identified *Candida* as a major fungus in tropospheric dust in north-eastern China, and it has been associated with the KD outbreak in Japan [7]. To date, three mouse models have been widely used to study the aetiology of vasculitis in KD: administration of a *Candida albicans* water-soluble fraction (CAWS), *Lactobacillus casei* cell wall extract (LCWE), and a synthetic Nod1 ligand [8–10]. While vasculitis observed in these murine models is similar to KD, Rodó et al. suggested that CAWS-induced vasculitis is suitable for studying the aetiology of KD [7].

Thrombomodulin (TM) (CD141) is an integral membrane protein expressed on the surface of endothelial cells, mesothelial cells, monocytes, and dendritic cell subsets, and serves as a cofactor for thrombin [11]. TM regulates blood coagulation by converting thrombin from a procoagulant enzyme to an anticoagulant enzyme. The thrombin-TM complex activates protein C to produce activated protein C (APC), which inactivates factors VIIIa and Va in the presence of protein S, thereby inhibiting further thrombin generation [12, 13]. Recombinant human soluble thrombomodulin (rTM) comprises the active extracellular domain of TM and inhibits blood coagulation by binding to thrombin [14, 15]. In addition, rTM has been used in Japan since 2008 for the treatment of disseminated intravascular coagulation (DIC), a severe thrombotic disease [16]. Interestingly, rTM has been reported to have anti-inflammatory and cytoprotective functions through both APC-dependent and -independent mechanisms [17, 18].

In this study, we used a mouse model of CAWS-induced vasculitis to investigate whether rTM could suppress the development of coronary arteritis. This is the first report to show potency of rTM against KD therapy.

Methods

Ethics statement

DBA/2 mice (male, 5 weeks old) were purchased from Japan SLC, Inc. (Tokyo, Japan). The mice were bred in an environment maintained at 23°C ± 1°C and 50% ± 10% relative humidity (3–6/cage); they had free access to feed and water. A light/dark cycle was maintained in which the lights were turned on from 8:00 to 20:00 h.

Preparation Of Caws

CAWS was prepared from *C. albicans* strain NBRC1385, which was acquired from the National Institute of Technology and Evaluation Biological Resource Center [10, 19]. Briefly, 5 L of completely synthetic medium (C-limiting medium) containing *C. albicans* was cultured in a glass incubator at 27°C for 2 days,

and air was supplied at a rate of 5 L/min. The culture was centrifuged at 400 rpm to remove *C. albicans*, and an equal amount of ethanol was added to the supernatant. The mixture was allowed to stand overnight, and then the precipitate was collected. The precipitate was dissolved in 250 mL of distilled water, and ethanol was added. The mixture was then left overnight. The resulting precipitate was collected and dried with acetone to obtain CAWS.

Effect Of Rtm On Caws-induced Vasculitis Model Of Mice

The rTM, prepared as previously reported [15], was supplied by Asahi-Kasei Pharma Co., Ltd. (Tokyo, Japan). CAWS-induced vasculitis was generated as previously described [10, 19]. Briefly, as shown in Fig. 1a, DBA/2 mice were intraperitoneally treated with CAWS (1 mg/mouse/day) for 5 consecutive days until day 0 of the experiment. The effects of rTM treatment on CAWS-induced vasculitis in mice were as follows: rTM was administered in two treatment intervals (Set A: 10 consecutive days from day 1 and Set B: 5 consecutive days from days 1 and 15) and four doses (0, 0.2, 1, and 4 mg/kg). For comparison, the mice were injected with 0.2 mL of phosphate-buffered saline for 2 weeks after CAWS treatment (CAWS-treated group). The mice were weighed and sacrificed by etherification on the indicated day. Autopsy was performed to obtain the heart and spleen, and both organs were weighed. Half of theses tissues were fixed in 10% neutralised formalin and the rest were stored in RNA later solution (QIAGEN NV, Limburg, Netherland)

Real-time Rt-pcr Analysis

Real-time RT-PCR analysis
The primer pairs used in this study are shown in Table 1. Total RNA was prepared from the heart and spleen using ISOGEN (Nippon Gene Co., Ltd., Toyama, Japan), according to the manufacturer's instructions. Real-time reverse transcription (RT)-PCR analysis was performed using StepOnePlus™ (Thermo Fisher Scientific, Inc., MA, USA) to detect mRNA expression. The expression level of the tested gene was normalised by subtracting the corresponding glyceraldehyde-3-phosphate dehydrogenase threshold cycle (CT) value. Normalisation was performed using the ΔΔCT comparison method.

Histopathological Analysis

The heart was immersed in 4% buffered paraformaldehyde overnight and replaced with 70% ethanol. The specimen was then placed on a tissue processor (ASP200; Leica Biosystems, Nußloch, Baden-Württemberg, Germany). The fixed specimen was replaced with the paraffin-impregnated specimen, and then embedded in a block of molten paraffin. The block was sectioned using a microtome (RM2125; Leica). The paraffin from the tissue on the slide was dissolved by Hemo-De (Leila) and ethanol treatment. The tissues were stained with haematoxylin and eosin (H&E) or Elastica van Gieson (EVG). The slides

were sealed and observed under an optimal microscope (BX51; Olympus Corporation, Tokyo Japan) at an appropriate magnification.

Statistical analysis

Student's *t*-test and the one-way analysis of variance (ANOVA) were used for comparisons between different study groups. GraphPad Prism 7 (GraphPad Software Inc., La Jolla, CA, USA) was used for statistical analysis.

Results

rTM treatment suppresses cardiac hypertrophy and arteritis in mice treated with CAWS

To investigate the effect of rTM on cardiac arteritis in a mouse model, the heart weight (HW) of CAWS-treated mice was measured, considering that cardiac hypertrophy is one of the typical observations in the CAWS-treated mice [20]. As shown in Fig. 1a, each dose of rTM was administered five times in a row on the designated day after CAWS treatment, and the HW of each mouse on day 34 was determined. There was no significant difference in body weight (BW) among the groups (the average BW in each group was 24.1–26.5 g, data not shown). As shown in Fig. 1b, the HW/BW ratio of the CAWS-treated mice significantly increased ($p < 0.01$) compared with that of the untreated mice, as reported previously [20]. The increased HW/BW of the CAWS-treated mice was reduced by treatment with rTM at both dosage intervals, demonstrating that rTM treatment suppressed the increase in HW, induced by CAWS treatment. Dosage intervals of Set A tended to suppress the increase in HW. The dosage intervals of Set B tended to suppress the increase in HW at all doses compared with that of Set A, and a significant suppression of increase in HW was observed at the highest dose of rTM (4 mg/kg), which was the same level as that of untreated mice. The suppression of HW/BW by the highest dose of rTM in Set B was similar to that shown in the previous study, in which the HW/BW ratio was reduced by IVIG (0.59 ± 0.07 at day 28) or etanercept (0.68 ± 0.07 at day 28) treatment in CAWS-treated mice [20].

Next, the effect of rTM on the development of aortic root vasculitis was histologically investigated using the highest dose of rTM (4 mg/kg). Both Elastica van Gieson staining and HE staining showed that the vascular structure of CAWS-treated mice was disrupted (Fig. 2, middle panel), compared with that of the untreated mice (Fig. 2, left panel). However, in CAWS-treated mice with rTM, the entire vascular structure was almost conserved, whereas hypertrophic vascular endothelium was developed (Fig. 2, right panel). Histological observations based on Elastica van Gieson staining also showed that fibrinoid necrosis occurred in CAWS-treated mice (Fig. 2, middle panel), whereas it was not observed in CAWS-treated mice administered rTM (Fig. 2, right panel). These results indicate that rTM treatment could suppress CAWS-induced coronary aneurysms.

Time course of inhibitory effect of rTM treatment on increased heart and spleen weights in mice treated with CAWS

As shown in Fig. 1, the dosage interval of rTM treatment for Set B more effectively suppressed the increase in the HW/BW ratio than Set A. Therefore, we adapted Set B as the regimen in the subsequent experiments. In addition to weighing the mouse heart, spleen weight (SW) was also measured as an indicator of suppression of inflammation in the whole mouse body at 20, 27, 34, and 48 days after CAWS treatment, with or without rTM. As shown in Fig. 3a, increasing the HW/BW ratio of CAWS-treated mice was supressed by rTM administration on day 27, although a significant difference was not calculated due to the high variation in the HW/BW ratio of CAWS-treated mice. The HW/BW ratio of CAWS-treated mice administered rTM remained the same as that of untreated mice on day 34. In contrast, the SW/BW ratio of CAWS-treated mice with rTM on day 20 was smaller than that of CAWS-treated mice, but higher than that of untreated mice. After day 27, the SW/BW ratio of mice treated with rTM increased to almost the same level as that of CAWS-treated mice (Fig. 3b), suggesting that the anti-inflammatory effect of rTM terminated within a week after the treatment in the whole body.

Histological changes associated with the time of cardioarteritis after rTM treatment

Histological examinations were performed to investigate the inhibitory effect of rTM on the development of vasculitis at the base of the aorta at several time points. On day 20, when histological changes are observed [10], there were no significant differences in the frequency of fibrinoid necrosis and elastic fibre destruction between CAWS-treated mice, with or without rTM administration. However, these changes were not observed in untreated mice (Fig. 4). On day 34, the histological observations were similar to those in Fig. 2 (data not shown). Fibrinoid necrosis and elastic fibre destruction were observed in CAWS-treated mice, depending on the HW/BW ratio, regardless of rTM treatment on day 48 (data not shown). These data suggest that rTM does not affect the induction of cardiac arteritis but may inhibit the development of cardiac arteritis.

Effect of rTM on the expression of genes associated with inflammation induced by CAWS

To investigate the underlying mechanism of rTM suppression in aortic root vasculitis, the expression of genes associated with inflammation were examined by RT-qPCR, using RNA extracted from the heart. On day 20, *IL-10* expression remained unchanged in the CAWS-treated mice compared with that in untreated mice, but *IL-10* expression in CAWS-treated mice administered rTM significantly increased ($p < 0.05$) compared with that in untreated mice and more significantly ($p < 0.0005$) compared with that in the CAWS-treated mice (Fig. 5a). The increased *IL-10* expression in CAWS-treated mice with rTM was observed until day 27 (Fig. 5b). Next, the gene expression levels of the inflammatory cytokines, interleukin 6 (IL-6) and TNF-α, were examined. These cytokines are enhanced in CAWS-treated mice and may be reduced by the administration of IVIG or etanercept [20]. When samples were prepared from mouse hearts on days 20 and 27, *IL-6* expression was not significantly different among the three groups (data not shown). Although no significant difference was observed in *TNF-α* expression among the three groups on

day 20 (Fig. 6a), but on day 27 *TNF-α* expression upregulated in samples from CAWS-treated mice not subjected to rTM treatment (Fig. 6b).

In addition, we examined the gene expression of other anti-inflammatory cytokines such as transforming growth factor beta (*TGF-β*) and interleukin-13 (*IL-13*) in the heart and spleen, but found no significant differences in gene expression among the groups of untreated mice, CAWS-treated mice, and CAWS-treated mice treated with rTM on days 20 and 27 (data not shown).

As described in Fig. 3b, rTM treatment suppressed the increase in the SW/BW ratio on day 20, but not on day 27. In addition, rTM treatment significantly increased *IL-10* expression in the heart of CAWS-treated mice on day 20. Therefore, we investigated the effect of rTM treatment on the expression of *IL-10* in the spleen on day 20. As shown in Fig. 7a, *IL-10* expression in the spleen of CAWS-treated mice was reduced compared with that in untreated mice, but its expression in CAWS-treated mice administered rTM was restored to the same level as in untreated mice. We also investigated the gene expression of thrombus-promoting tissue factor (*TF*), which induces thrombus formation and DIC, and may be associated with the significant ($p < 0.0005$) increase in the SW/BW due to spleen hypertrophy in CAWS-treated mice on day 20, as shown in Fig. 3b. *TF* expression in the spleen of the CAWS-treated mice was significantly increased ($p < 0.05$) compared with that in untreated mice, and the increased *TF* expression in the spleen of CAWS-treated mice was significantly ($p < 0.01$) decreased to the same level as in untreated mice by treatment with rTM (Fig. 7b). These results suggest that rTM could regulate the inflammatory activation of coagulation and tissue remodelling, as reported by a study performed using a human endothelial microfluidic model [21]. No significant difference in spleen *IL-10* and *TF* expression was observed compared with that in samples of CAWS-treated mice administered rTM and mice not administered rTM, consistent with the SW/BW ratio on day 27 (data not shown).

Discussion

KD is characterised by coronary vasculitis, followed by an aneurysm, which can lead to the development of coronary artery aneurysms if left untreated with IVIG therapy, the standard treatment for acute KD. However, 10–20% of patients are resistant to IVIG therapy and are at an increased risk of coronary vasculitis. In addition, the relative roles of second IVIG infusion, corticosteroids, calcineurin inhibitors, and interleukin-1 antagonists remain controversial [22]. Recent studies have demonstrated favourable effects of rTM on experimental and clinical DIC associated with sepsis, acute promyelocytic leukaemia, and other diseases associated with vascular inflammation and blood coagulation [14, 15, 18]. rTM exhibits anti-inflammatory properties in addition to anticoagulant properties. In fact, the C-type lectin-like domain of TM, which lacks the thrombin-binding ability, inhibits the alamin high-mobility group box 1 protein [23] and lipopolysaccharide (LPS) [24] and suppresses neutrophil adhesion to endothelial cells [17], during which rTM promotes the inhibition of the mitogen-activated protein kinase pathway and activation of nuclear factor-κB [17]. Recently, Okamoto et al. [25] demonstrated the mechanism underlying rTM inhibition of monocyte adhesion to endothelial cells by suppressing LPS-induced cell sclerosis in a cell stiffness-dependent manner. This may reduce endothelial inflammation and atherosclerosis.

Thus, in this study, we investigated whether rTM has a suppressive effect on the development of KD-related coronary vasculitis using a CAWS-induced mouse model of KD. Treatment with rTM suppressed inflammation of the heart and spleen of KD model mice and alleviated hypertrophy (Figs. 1, 2, and 3). The time lag of dilation between the heart and spleen indicated that the process of vascular inflammation is a slow event in this mouse model. Although rTM treatment reduced vascular inflammation, rTM treatment did not completely cure the inflammation or improve the death rate of CAWS-treated mice. Given the half-life of rTM and the time limit for suppressing spleen hypertrophy (Fig. 3), it may be beneficial to repeat the 5-day rTM treatment, followed by a 9-day discontinuation cycle.

The gene expression analysis suggested that rTM induces IL-10 production and suppresses TF production, resulting in the suppression of aortic root and coronary artery inflammation, vasculitis, and fibrosis in the heart and spleen (Figs. 5, 6, and 7). However, there were no significant differences in the gene expression of anti-inflammatory cytokines, *TGF-β* and *IL-13*, among groups of untreated mice, CAWS-treated mice, and CAWS-treated mice administered rTM on days 20 and 27. Therefore, rTM may specifically induce IL-10 production and suppress TF production. Further research is needed to elucidate the underlying mechanism of KD-related vasculitis and the effectiveness of rTM for KD, but a similar hypothesis that IL-10 prevents vasculitis in a CAWS-induced mouse model has been reported [9, 19]. Interestingly, the serum IL-10 level was elevated in CAWS-resistant CBA/J mice after CAWS treatment, but not in CAWS-sensitive strains, namely, C57BL/6, C3H/HeN, and DBA/2 mice. In addition, Nakamura et al. demonstrated a significant reduction in aortic root and coronary vascular inflammation and fibrosis in CAWS-treated mice injected with adeno-associated virus-mediated IL-10 [26]. A previous study also showed that the level of IL-10 was increased in rTM-treated dendric cells, whereas the proportion of inflammatory cytokines was low [27]. In addition, IL-10 induction was observed in mouse lungs following rTM treatment (severe acute respiratory distress syndrome) and spleen (hematopoietic SCT model) [28, 29].

Several clinical trials have been conducted to examine the feasibility of the clinical application of IL-10. Supplementation of recombinant human IL-10 in patients with psoriasis provided showed clinical improvements but failed to improve Crohn's disease and rheumatoid arthritis [30, 31, 32]. The serious adverse effects of IL-10 therapy are anaemia and thrombocytopaenia. However, the adverse effects of rTM treatment are controllable, and rTM acts especially on vascular endothelial cells, whereas IL-10 treatment directly affects cells associated with the immune system and inflammation, making rTM useful for treating KD. Thus, rTM may be an alternative to IL-10 production.

Certain inflammatory cytokines, most importantly TNF-α, are implicated in the pathogenesis of KD [2, 20]. In fact, anti-TNF-α drugs, such as the chimeric murine/human immunoglobulin G1 monoclonal antibody infliximab, have been shown to be effective in treating patients with KD who are refractory to initial IVIG therapy. In this study, rTM treatment did not alter the production of TNF-α or the induction of cardiac arteritis (Figs. 4 and 6). Therefore, combination therapy with rTM and anti-TNF-α drugs may be effective in controlling KD coronary arteritis.

Epidemiologic studies have reported that healthy individuals who maintain high plasma thrombomodulin levels are at a low risk of developing coronary artery syndrome [33, 34]. In addition, rTM neutralises histones, which are major extracellular mediators of death, and reduces fatal thrombosis, in mice [35], and this is consistent with our findings. Therefore, rTM may be an alternative treatment strategy for KD as it induces IL-10 production and prevents histone-induced thrombosis.

It has been reported that patients with corona virus disease 2019 (COVID-19) infected with the mutant coronavirus (severe acute respiratory syndrome corona virus 2: SARS-CoV-2) present primarily with acute respiratory distress syndrome and, in some cases, multiple organ failure caused by abnormal coagulation and thrombosis [36]. Guglielmetti et al. illustrated the association between thrombotic-induced inflammation and multiple organ endothelial dysfunction in patients with COVID-19, and proposed therapeutic strategies to improve microangiopathy and mitigate symptoms by treating with drugs other than heparin, such as rTM and nafamostat mesylate [37]. Paediatric patients with COVID-19 exhibit hyperinflammatory and/or KD-like symptoms and have been treated with IVIG, acetylsalicylic acid, tocilizumab, anakinra, enoxaparin, and methylprednisolone [38]. Treatment with rTM may also be effective against KD-like symptoms and thrombotic disease in patients with COVID-19, and this warrants further investigation.

Conclusions

The findings of this study suggested that rTM induces IL-10 production, reduces TF production, and prevents vascular inflammation and fibrosis in a mouse model of KD. These results suggest the potential applications of rTM treatment in patients with KD and provide new insights into the underlying mechanisms of KD aetiology.

Abbreviations

APC: activated protein C; BW: body weight; CAWS: *Candida albicans* water-soluble fraction; COVID-19: corona virus disease 2019; EVG: Elastica van Gieson; H□E: haematoxylin and eosin; HW: heart weight; IVIG: Intravenous immunoglobulin; IL-6: interleukin-6; IL-10: interleukin-10; IL-13: interleukin-13; KD: Kawasaki disease; LCWE: Lactobacillus casei cell wall extract; LPS: lipopolysaccharide; RT: reverse transcription; rTM: recombinant human soluble thrombomodulin; SARS-CoV-2: severe acute respiratory syndrome corona virus 2; SW: spleen weight; TM: thrombomodulin; TF: tissue factor; TNF-α: tumour necrosis factor alpha; TGF-β: transforming growth factor beta

Declarations

Ethics approval and consent to participate

All experiments in this study were approved by the Laboratory Animal Use and Care Committee of the Suzuka University of Medical Science Laboratory Animal Use Guide (License No. 30) and conducted in

accordance with the guidelines of Suzuka University of Medical Science.

Consent for publication

Not applicable.

Availability of data and materials

All the important data are provided in the paper. The datasets used and/or analysed during the current study are available from the corresponding authors upon reasonable request.

Competing interests

The author declares that there are no competing interests.

Funding

This research was partially supported by funding from the Japan Society for the Promotion of Science (JSPS) (grant numbers JP16K08633, JP16K08791 and JP19K08850), and rTM was provided by Asahi-Kasei Pharma Co., Ltd. (Tokyo, Japan).

Author contributions

HN and KS designed the research concepts and experiments and wrote the manuscript. HN, HI, KK, TI, KH, and TT conducted experiments and analysed the data. N-NM, YA, and NO produced CAWS. HI and TI discussed the data and helped draft the manuscript.

Acknowledgement

We thank Ms. Eku Adachi, Dr. Keigo Nishida, and Dr. Keigo Ueno, who provided technical support and useful information. Recombinant human soluble TM (rTM) was supplied by Asahi-Kasei Pharma Co., Ltd. (Tokyo, Japan).

References

1. Kawasaki T, Kosaki F, Okawa S, Shigematsu I, Yanagawa H. A new infantile acute febrilemucocutaneous lymph node syndrome (MLNS) prevailing in Japan. Pediatrics. 1974;54:271–6.
2. Newburger JW, Takahashi M, Burns JC. Kawasaki disease. J Am Coll Cardiol. 2016;67:1738–49.
3. Denby KJ, Clark DE, Markham LW. Management of Kawasaki disease in adults. Heart. 2017;103:1760–9.
4. Burns JC, Franco A. The immunomodulatory effects of intravenous immunoglobulin therapy in Kawasaki disease. Expert Rev Clin Immunol. 2015;11:819–25.

5. Son MB, Gauvreau K, Burns JC, Corinaldesi E, Tremoulet AH, Watson VE, Baker A, Fulton DR, Sundel RP, Newburger JW. Infliximab for intravenous immunoglobulin resistance in Kawasaki disease: a retrospective study. J Pediatrics. 2011;158:644–9.
6. Frazer J. Infectious disease: blowing in the wind. Nature. 2012;484:21–3.
7. Rodó X, Curcoll R, Robinson M, Ballester J, Burns JC, Cayan DR, Lipkin WI, Williams BL, Couto-Rodriguez M, Nakamura Y, et al. Tropospheric winds from northeastern China carry the etiologic agent of Kawasaki disease from its source to Japan. Proc Natl Acad Sci USA. 2014;111:7952–7.
8. Motomura Y, Kanno S, Asano K, Tanaka M, Hasegawa Y, Katagiri H, Saito T, Hara H, Nishio H, Hara T, et al. Identification of pathogenic cardiac CD11c + macrophages in Nod1-mediated acute coronary arteritis mediated acute coronary arteritis. Arterioscler Thromb Vasc Biol. 2015;35:1423–33.
9. Lee Y, Schulte DJ, Shimada K, Chen S, Crother TR, Chiba N, Fishbein MC, Lehman TJA, Arditi M. Interleukin-1beta is crucial for the induction of coronary artery inflammation in a mouse model of Kawasaki disease. Circulation. 2012;125:1542–50.
10. Nagi-Miura N, Shingo Y, Adachi Y, Ishida-Okawara A, Oharaseki T, Takahashi K, Naoe S, Suzuki K, Ohno N. Induction of coronary arteritis with administration of CAWS (*Candida albicans* water-soluble fraction) depending on mouse strains. Immunopharmacol Immunotoxicol. 2004;26:527–43.
11. Esmon NL, Owen WG, Esmon CT. Isolation of a membrane-bound cofactor for thrombin-catalyzed activation of protein C. J Biol Chem. 1982;257:859–64.
12. Esmon CT, Owen WG. The discovery of thrombomodulin. J Thromb Haemost. 2004;2:209–13.
13. Suzuki K, Nishioka J, Matsuda M, Hashimoto S. Protein S is essential for activated protein C-catalyzed inactivation of platelet-associated Factor Va. J Biochem. 1984;96:455–95.
14. Suzuki K, Kusumoto H, Deyashiki Y, Nishioka J, Maruyama I, Zushi M, Kawahara S, Honda G, Yamamoto S, Horiguchi S. Structure and expression of human thrombomodulin, a thrombin receptor on endothelium acting as a cofactor for protein C activation. EMBO J. 1987;6:1891–7.
15. Suzuki K, Hayashi T, Nishioka J, Kosaka Y, Zushi M, Honda S, Yamamoto S. A domain composed of epidermal growth factor-like structures of human thrombomodulin is essential for thrombin binding and for protein C activation. J Biol Chem. 1989;264:4872–6.
16. Saito H, Maruyama I, Shimazaki S, Yamamoto Y, Aikawa N, Ohno R, Hirayama A, Matsuda T, Asakura H, Nakashima M, et al. Efficacy and safety of recombinant human soluble thrombomodulin (ART-123) in disseminated intravascular coagulation: results of a phase III, randomized, double-blind clinical trial. J Thromb Haemost. 2007;5:31–41.
17. Conway EM, Van de Wouwer M, Pollefeyt S, Jurk K, Van Aken H, De Vriese A, Weitz JI, Weiler H, Hellings PW, Schaeffer P, et al. The lectin-like domain of thrombomodulin confers protection from neutrophil-mediated tissue damage by suppressing adhesion molecule expression via nuclear factor kappaB and mitogen-activated protein kinase pathways. J Exp Med. 2002;196:565–77.
18. Abeyama K, Stern DM, Ito Y, Kawahara K, Yoshimoto Y, Tanaka M, Uchimura T, Ida N, Yamazaki Y, Yamada S, et al. The N-terminal domain of thrombomodulin sequesters high-mobility group-B1 protein, a novel antiinflammatory mechanism. J Clin Invest. 2005;115:1267–74.

19. Nagi-Miura N, Komai M, Adachi Y, Osada N, Kameoka Y, Suzuki K, Ohno N. IL-10 is a negative regulatory factor of CAWS-vasculitis in CBA/J mice as assessed by comparison with Bruton's tyrosine kinase-deficient CBA/N mice. J Immunol. 2009;183:3417–24.
20. Ohashi R, Fukuzawa R, Watanabe M, Tajima H, Nagi-Miura N, Ohno N, Tsuchiya S, Fukuda Y, Ogawa S, Itoh Y. Etanercept suppresses arteritis in a murine model of kawasaki disease: a comparative study involving different biological agents. Int J Vasc Med. 2013;2013:543141.
21. Greineder CF, Johnston IH, Villa CH, Gollomp K, Esmon CT, Cines DB, Poncz M, Muzykantov VR. ICAM-1-targeted thrombomodulin mitigates tissue factor-driven inflammatory thrombosis in a human endothelialized microfluidic model. Blood Adv. 2017;1:1452–65.
22. Galeotti C, Kaveri SV, Cimaz R, Kone-Paut I, Bayry J. Predisposing factors, pathogenesis and therapeutic intervention of Kawasaki disease. Drug Discov Today. 2016;21:1850–7.
23. Ito T, Kawahara K, Okamoto K, Yamada S, Yasuda M, Imaizumi H, Nawa Y, Meng X, Shrestha B, Hashiguchi T, et al. Proteolytic cleavage of high mobility group box 1 protein by thrombin-thrombomodulin complexes. Arter Thromb Vasc Biol. 2008;28:1825–30.
24. Ma CY, Chang WE, Shi GY, Chang BY, Cheng SE, Shih YT, Wu HL. Recombinant thrombomodulin inhibits lipopolysaccharide-induced inflammatory response by blocking the functions of CD14. J Immunol. 2015;194:1905–15.
25. Okamoto T, Kawamoto E, Usuda H, Tanaka T, Nikai T, Asanuma K, Suzuki K, Shimaoka M, Wada K. Recombinant human soluble thrombomodulin suppresses monocyte adhesion by reducing lipopolysaccharide-induced endothelial cellular stiffening. Cells. 2020;9:1811.
26. Nakamura J, Watanabe S, Kimura H, Kobayashi M, Karasawa T, Kamata R, Usui-Kawanishi F, Sadatomo A, Mizukami H, Nagi-Miura N, et al. Adeno-associated virus vector-mediated interleukin-10 induction prevents vascular inflammation in a murine model of Kawasaki disease. Sci Rep. 2018;8:7601.
27. Toda M, Shao Z, Yamaguchi KD, Takagi T, D'Alessandro-Gabazza CN, Taguchi O, Salamon H, Leung LLK, Gabazza EC, Morser J. Differential gene expression in thrombomodulin (TM; CD141)(+) and TM(-) dendritic cell subsets. PLoS One. 2013;8:e72392.
28. Kudo D, Toyama M, Aoyagi T, Akahori Y, Yamamoto H, Ishii K, Kanno E, Maruyama R, Kaku M, Kushimoto S, et al. Involvement of high mobility group box 1 and the therapeutic effect of recombinant thrombomodulin in a mouse model of severe acute respiratory distress syndrome. Clin Exp Immunol. 2013;173:276–87.
29. Ikezoe T, Yang J, Nishioka C, Yokoyama A. Thrombomodulin alleviates murine GVHD in association with an increase in the proportion of regulatory T cells in the spleen. Bone Marrow Transplant. 2015;50:113–20.
30. Ng TH, Britton GJ, Hill EV, Verhagen J, Burton BR, Wraith DC. Regulation of adaptive immunity; the role of interleukin-10. Front Immunol. 2013;4:129.
31. Castillo P, Kolls JK. IL-10: A paradigm for counterregulatory cytokines. J Immunol. 2016;197:1529–30.

32. Saxena A, Khosraviani S, Noel S, Mohan D, Donner T, Hamad AR. Interleukin-10 paradox: A potent immunoregulatory cytokine that has been difficult to harness for immunotherapy. Cytokine. 2015;74:27–34.
33. Blann AD, Amiral J, McCollum CN. Prognostic value of increased soluble thrombomodulin and increased soluble E-selectin in ischemic heart disease. Eur J Haematol. 1997;59:115–20.
34. Blann AD, Seigneur M, Steiner M, Boisseau MR, McCollum CN. Circulating endotherial markers in perpheral vascular disease relationship to the location and extent of atherosclerotic disease. Eur J Clin Invest. 1997;27:916–21.
35. Nakahara M, Ito T, Kawahara K, Yamamoto M, Nagasato T, Shrestha B, Yamada S, Miyauchi T, Higuchi K, Takenaka T, et al. Recombinant thrombomodulin protects mice against histone-induced lethal thromboembolism. PLoS One. 2013;8:e75961.
36. Levi M, Thachil J, Iba T, Levy JH. Coagulation abnormalities and thrombosis in patients with COVID-19. Lancet Haematol. 2020;7:e438-40.
37. Guglielmetti G, Quaglia M, Sainaghi PP, Castello LM, Vaschetto R, Pirisi M, Corte FD, Avanzi GC, Stratta P, Cantaluppi V. “War to the knife” against thromboinflammation to protect endothelial function of COVID-19 patients. Crit Care. 2020;24:365.
38. Akca UK, Kesici S, Ozsurekci Y, Aykan HH, Batu ED, Atalay E, Demir S, Sag E, Vuralli D, Bayrakci B, et al. Kawasaki-like disease in children with COVID-19. Rheumatol Int. 2020;40:2105–15.

Tables

Due to technical limitations, table 1 is only available as a download in the Supplemental Files section.

Figures

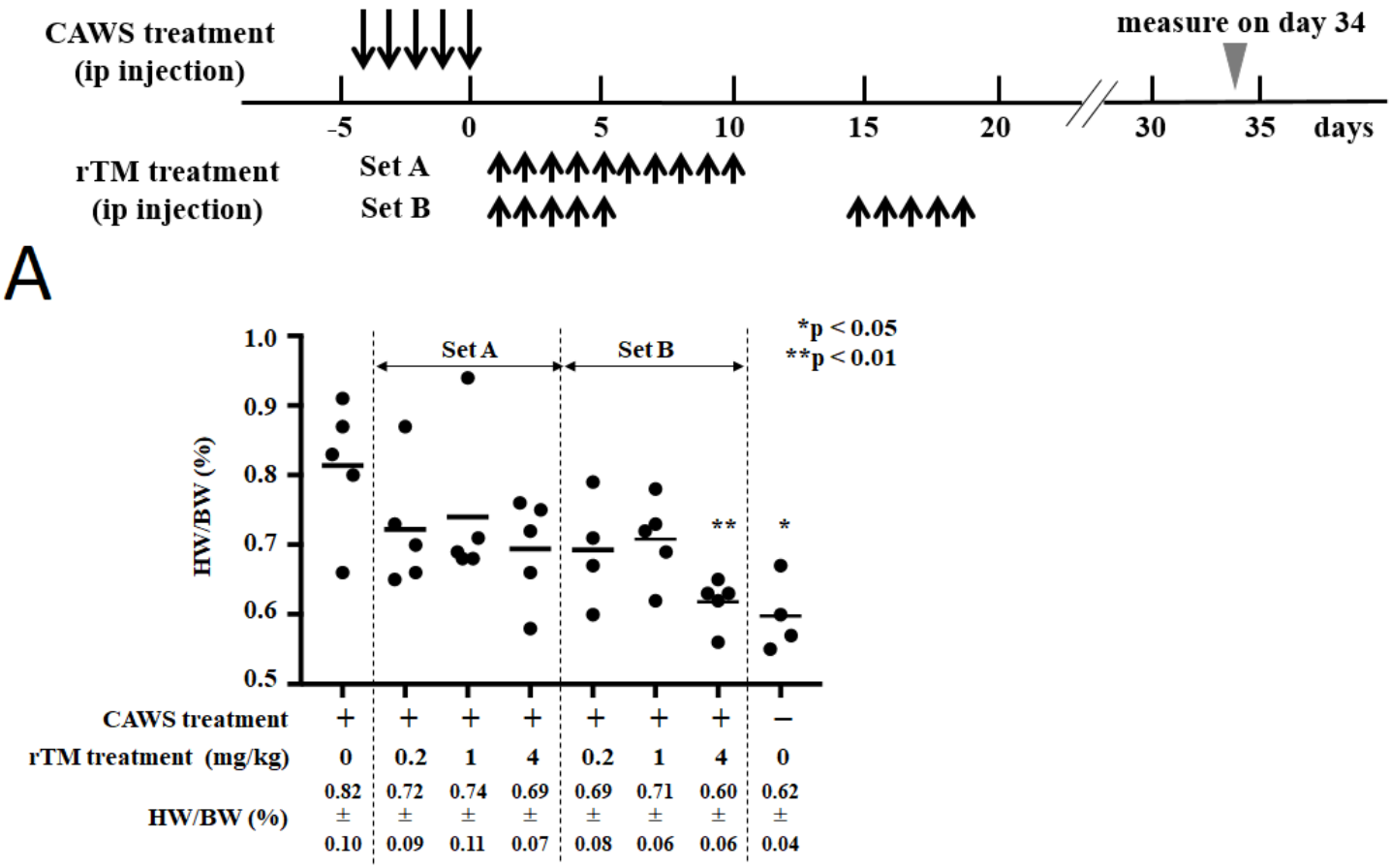

Figure 1

Effect of rTM on cardiac hypertrophy in a mouse KD model. (a) Schematic treatment of dosage regimens of rTM and CAWS in male DBA/2 mice (4-week-old). (b) The inhibitory effect of rTM on increased HW/BW (heart weight per body weight) due to cardiac hypertrophy induced by CAWS treatment. Mice were sacrificed 34 days after CAWS treatment, and the resected hearts were weighed. *p < 0.05, **p < 0.01 using the one-way analysis of variance (ANOVA). Repeated experiments showed almost the same results.

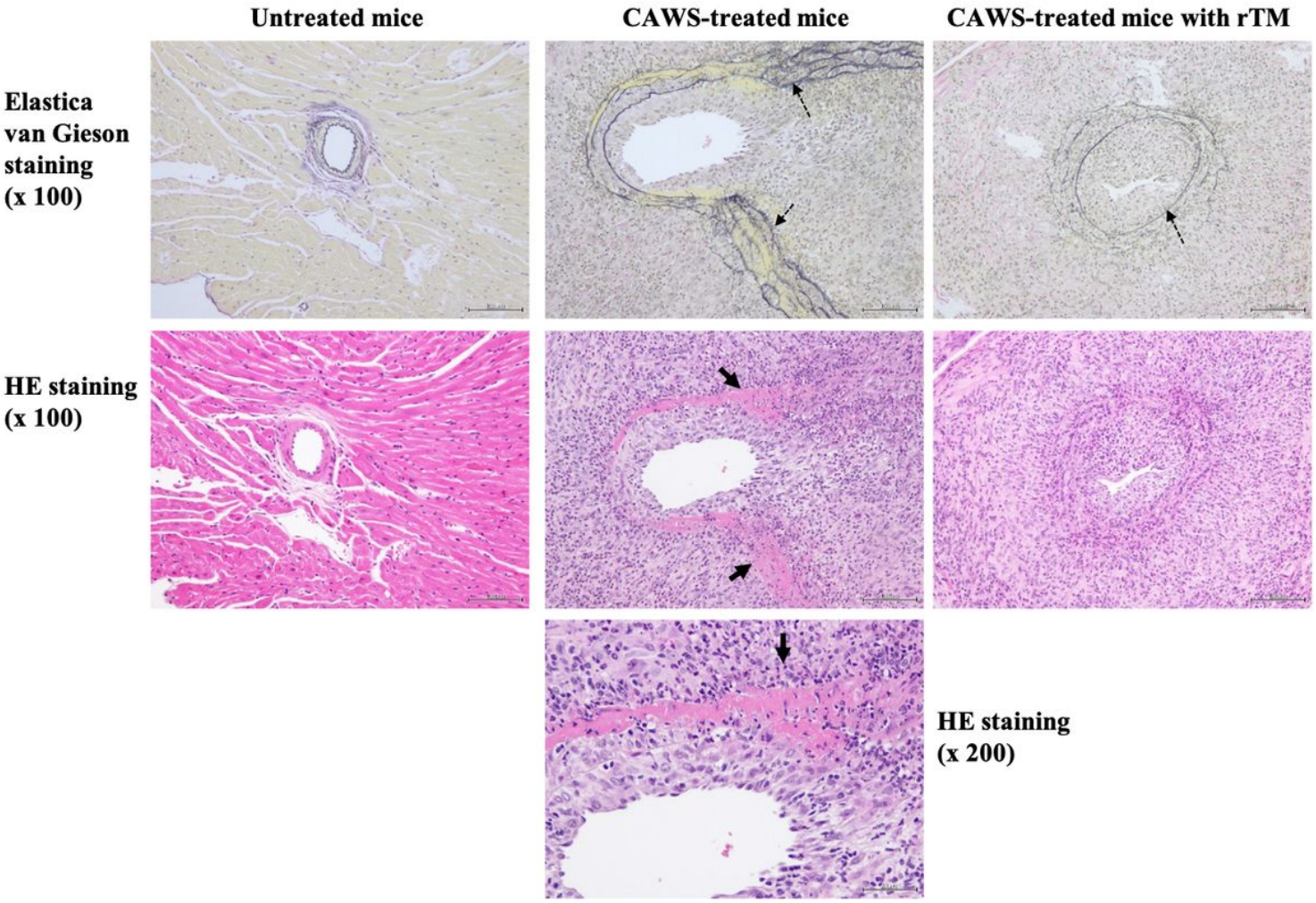

Figure 2

Histological observations on the development of vasculitis in aortic roots in mice. Upper panels show Elastica van Gieson staining (magnification: 100×), middle and lower panels show HE staining (middle panels; magnification: 100×, lower panel; 200×). Dashed arrows show lamina elastica in the heart of mice treated with CAWS. Arrows show fibrinoid necrosis in the heart. Left panels show the sample prepared from untreated mice. Middle panels show the sample prepared from CAWS-treated mice. The right panels show the sample prepared from CAWS-treated mice administered rTM (4 mg/kg).

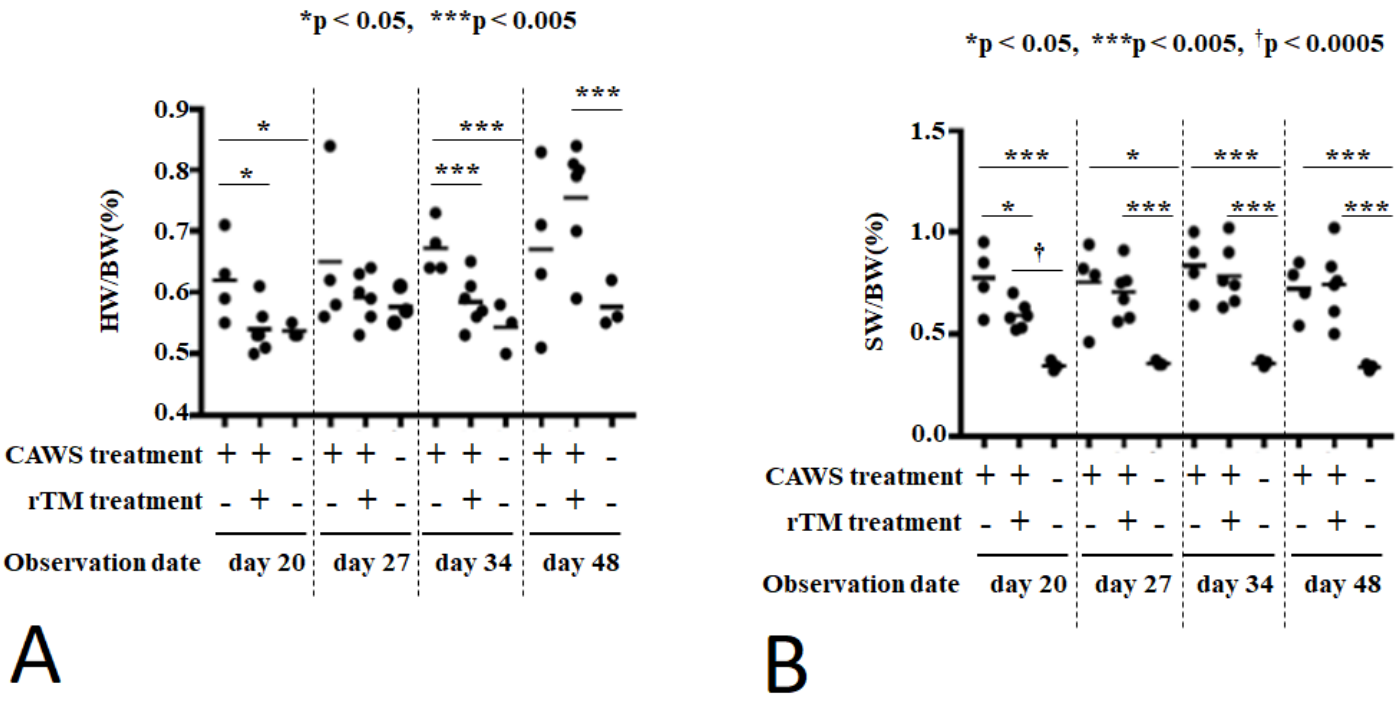

Figure 3

Weight variation of heart (a) and spleen (b) after treatment with rTM. After treatment with rTM (4 mg/kg) at 5 consecutive days from days 1 and 15, whole body, heart, and spleen were weighed on days 20, 27, 34, and 48. *p < 0.05, ***p < 0.005, and †p < 0.0005 by Student's t-test between the groups on the same date. Repeated experiments showed similar results.

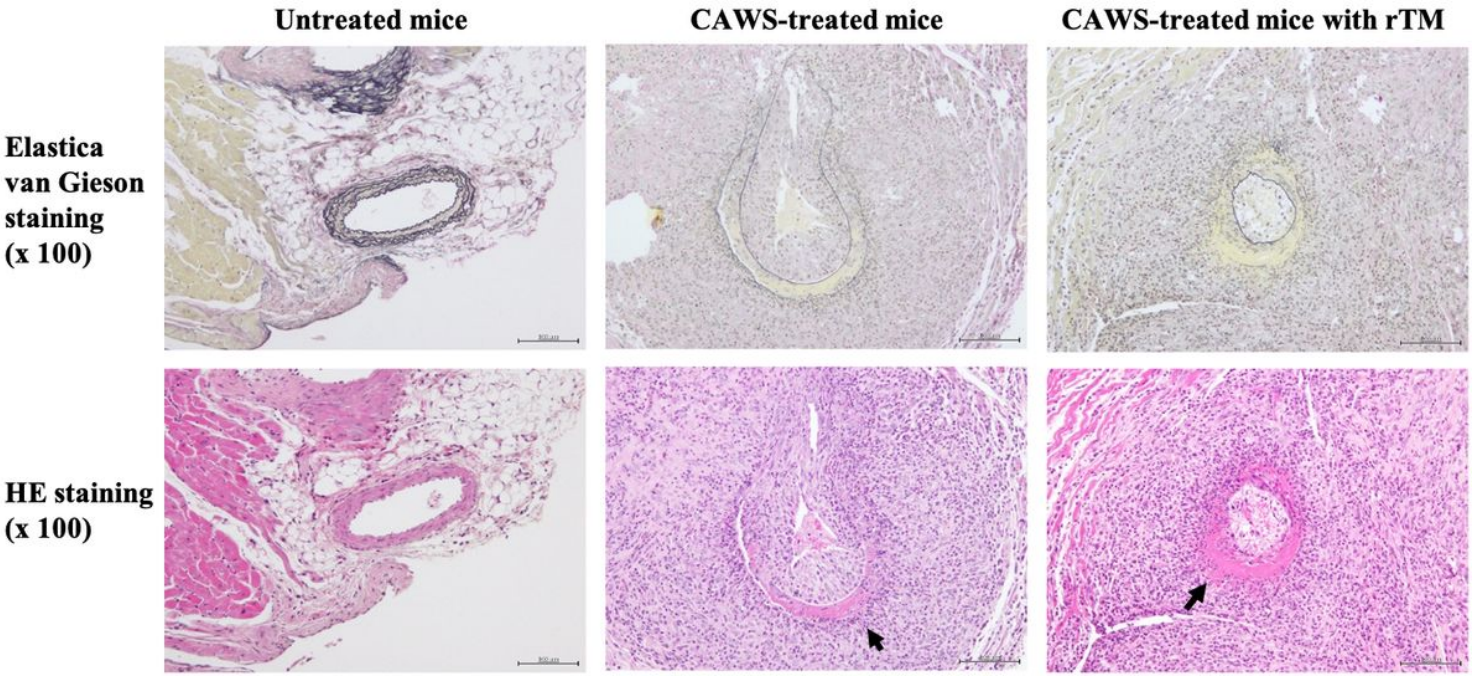

Figure 4

Histological observations of the inhibitory effect of rTM on developing vasculitis in aortic roots. The samples were prepared from the tissues dissected on day 20. Upper panels show Elastica van Gieson staining (magnification: 100×), lower panels show HE staining (magnification: 100×). Arrows show fibrinoid necrosis in the heart of CAWS-treated mice. Left panels show the sample prepared from untreated mice. Middle panels show the sample prepared from CAWS-treated mice. Right panels show the sample prepared from CAWS-treated mice with rTM (4 mg/kg).

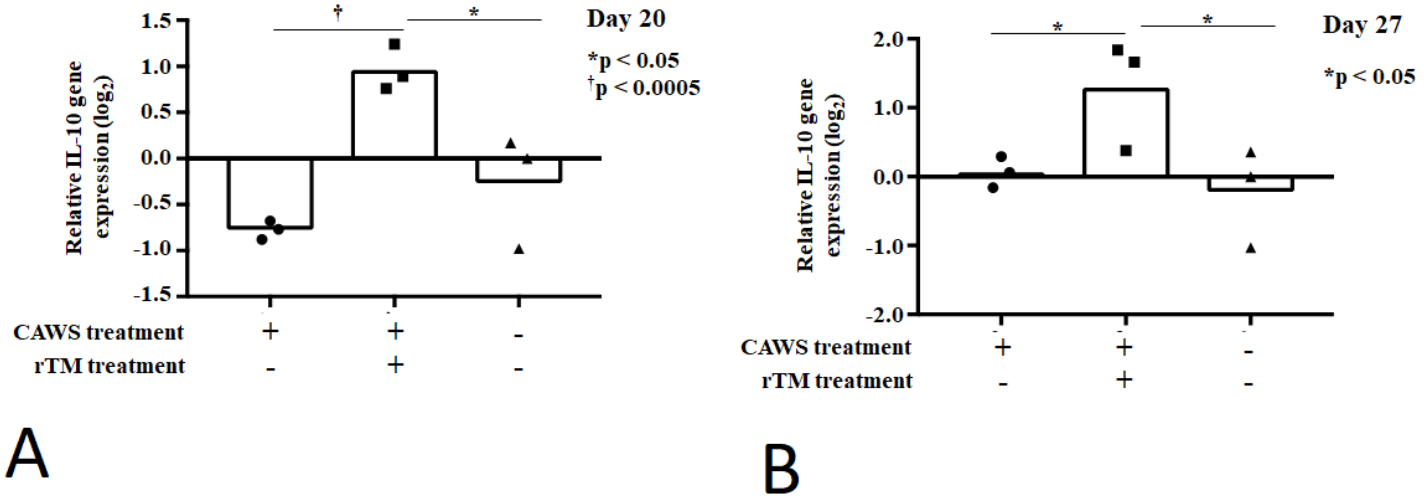

A B

Figure 5

Schematic IL-10 expression in the heart on day 20 (a) and day 27 (b). The expression level was compared with that of sample from untreated mice. †p < 0.0005 using Student's t-test between CAWS-treated mice treated with and without rTM, *p < 0.05 using Student's t-test between untreated mice and CAWS-treated mice or between CAWS-treated mice and CAWS-treated mice administered rTM. Repeated experiments showed similar results.

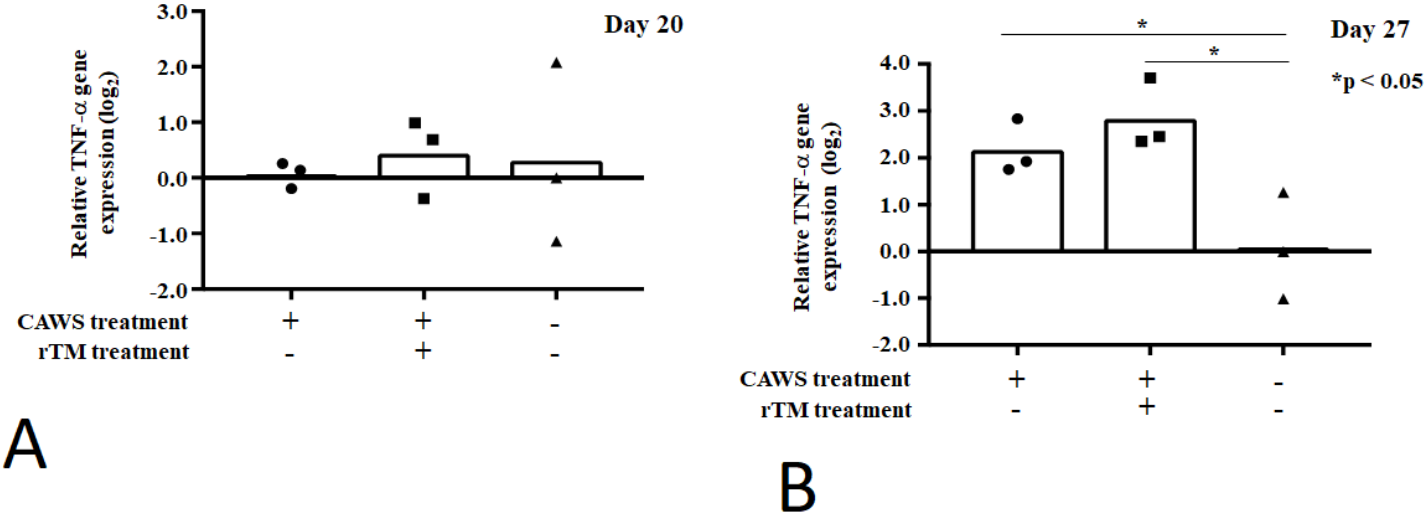

A B

Figure 6

Schematic TNF-α expression in the heart on day 20 (a) and day 27 (b). The expression level was compared with that that in sample from untreated mice. *p < 0.05 using Student's t-test between CAWS-treated mice and CAWS-treated mice treated with rTM or between CAWS-treated mice treated with rTM and untreated mice. Repeated experiments showed similar results.

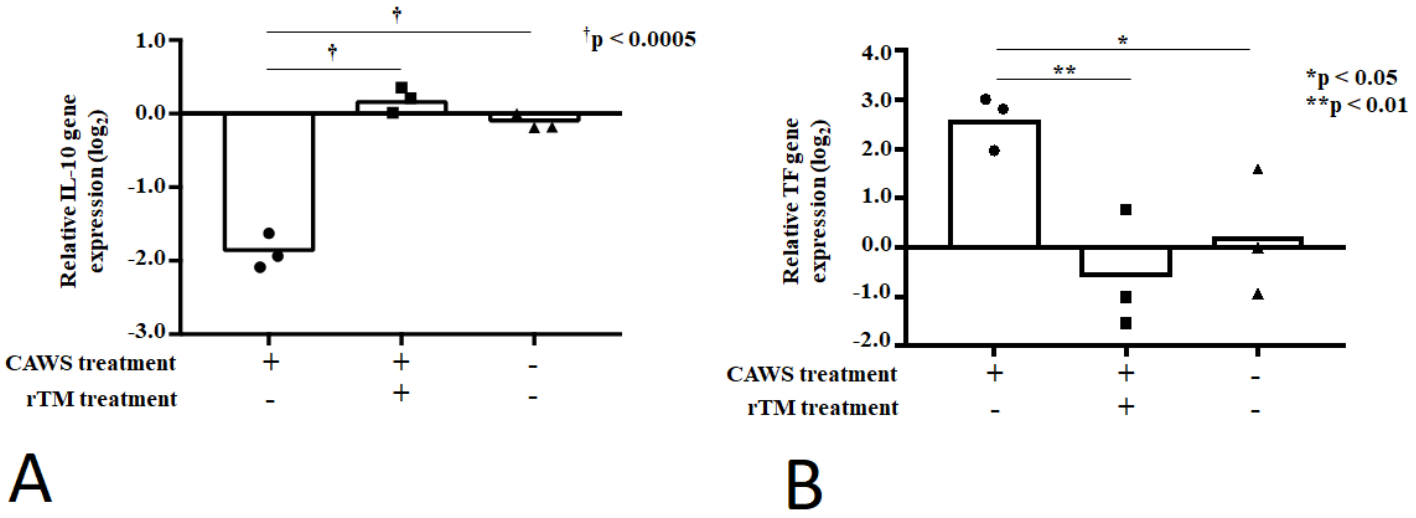

Figure 7

Schematic IL-10 (a) expression in the heart and TF (b) expression in the spleen. The RNA was isolated from the tissues dissected on day 20. The expression level was compared with that in sample from untreated mice. *p < 0.05, **p < 0.01, and †p < 0.0005 using Student's t-test between CAWS-treated mice and untreated mice or CAWS-treated mice administered rTM. Repeated experiments showed similar results.

Supplementary Files

This is a list of supplementary files associated with this preprint. Click to download.

- table10228.xlsx